Spectral Shaping Technology and its Application for Dense-Gas Dessert Prediction on Songliao Basin

Hong-wei Deng, Yi Bao(✉), Jiang-yun Pei, Hui-tian Lan, and Ji-feng Ding

Seismic Data Processing and Interpretation Center, Exploration and Development Research Institute of Daqing Oilfield Company Ltd. CNPC, Ranghulu District, Daqing 163712, Heilongjiang, China
baoyi6@petrochina.com.cn

Abstract. In Anda-Songzhan area, the dense sandy gravel of Shahezi formation is generally gas-bearing, which is a key field of natural-gas reserve replacement in Songliao Basin. However, the resolution of deep seismic data is low, so it is difficult to meet the accuracy requirements of dessert prediction in unconventional reservoirs. On the basis of amplitude-preserving imaging processing, we count the global wavelet for poststack anti-Q filtered seismic records, get the global filter operator by shaping the global wavelet with the expected output wavelet, and obtain the seismic records of frequency extension by making convolution the operator with the poststack data. After processing, the main frequency of data is increased by 14 Hz, and the average coincidence rate of sandstone “dessert area” selected by combining multiple attributes with relative wave impedance inversion is increased from 67 to 80%. It supports the deployment of 7 exploration wells in this area and provides strong technical support for increasing storage and production in unconventional fields.

Keywords: Unconventional reservoirs · Spectral shaping · Desserts prediction · Songliao Basin · Dense gas

This paper was prepared for presentation at the 2018 International Field Exploration and Development Conference in Xi’an, China, 18–20 September, 2018.

J. Lin (ed.), *Proceedings of the International Field Exploration and Development Conference 2018*, Springer Series in Geomechanics and Geoengineering, https://doi.org/10.1007/978-981-13-7127-1_49

1 Introduction

The successive success of well S9 and well S12 in Anda-Songzhan area reveals a good prospect for exploration of dense sandy gravel gas in the deep Shahezi formation and will also become a key field for the replacement of deep gas reserves in Songliao Basin. Due to the complexity of the gas reservoir itself, the exploration and deployment are still facing with a series of difficulties, although some progress has been made in seismic exploration of deep dense sandy gravel gas reservoirs. After two acquisitions and multiple rounds of processing, the imaging accuracy and resolution of deep seismic data are still difficult to meet the requirements of subdivision layer structural interpretation and reservoir prediction accuracy, and this directly leads to unclear understanding of sedimentary facies and reservoir distribution, which results in difficult prediction of desserts. As shown in Fig. 1, the latest collected data after processing has low vertical resolution and the main frequency is about 25 Hz. According to the empirical algorithm with vertical resolution of about 1/4 wavelength, the vertical resolution of the data is about 40–50 m. The seismic identification of single sand body is difficult, and there are some problems such as insufficient seismic imaging accuracy, unclear fault breakpoints between layers, low signal-to-noise ratio of data and unclear relationship between some formation reflection wave groups. The full coverage area of the research area is 200 km^2, and the period of dessert prediction is short. Therefore, a processing method with good effect frequency extension and efficient in computation must be found to improve the quality of seismic data.

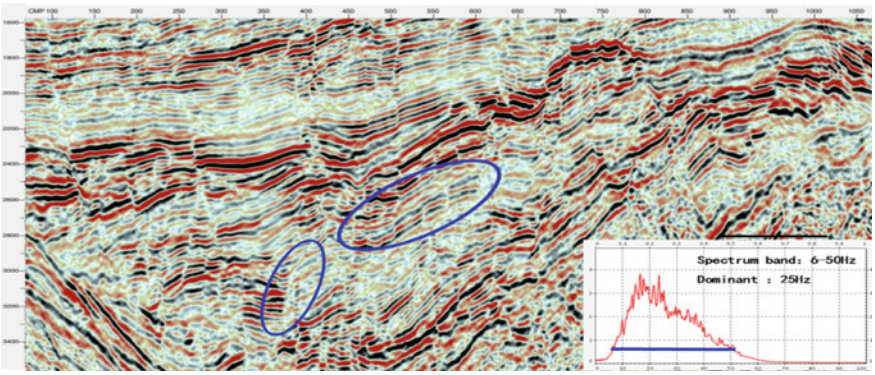

Fig. 1. RTM migration section in Anda-Songzhan (Line_262)

2 Principles

There are many methods to improve the vertical resolution of seismic data, such as inverse Q filter, spectral decomposition technique represented by generalized S transform, spectrum shaping technique and prestack time migration technology of viscoelastic media unique to Daqing Research Institute, etc. The following is a brief description of the principles of these techniques.

3 Inverse Q filter

When plane wave propagates in viscoelastic medium, the analytical solution of one-pass wave is as follows:

$$P(z+\Delta z,\omega) = P(z,\omega)\exp[-jk(\omega)\Delta z] \tag{1}$$

where z is depth, j is imaginary unit, ω is angular frequency, where the Q effect of the formation can be introduced by the complex number wave $k(\omega)$:

$$k(\omega) = \frac{\omega}{\upsilon_{\mathrm{r}}}\left(1 - \frac{j}{2Q_{\mathrm{r}}}\right)\left(\frac{\omega}{\omega_{\mathrm{h}}}\right)^{-r} \tag{2}$$

where, Q_{r} and υ_{r} are the quality factor and phase velocity of the reference frequency, ω_{h} is the tuning parameter, $r = 1/\pi Q$. Therefore, the inverse Q filter results can be expressed as,

$$\begin{aligned} P(\tau+\Delta\tau,\omega) = P(\tau,\omega)\exp\left[\left(\frac{\omega}{\omega_{\mathrm{h}}}\right)^{-\mathrm{r}}\frac{\omega\Delta\tau}{2Q_{\mathrm{r}}}\right] \\ \times\ \exp\left[-j\left(\frac{\omega}{\omega_{\mathrm{h}}}\right)^{-r}\omega\Delta\tau\right] \end{aligned} \tag{3}$$

when the Q value varies continuously with the travel time, the surface wave field can be extended to the time depth τ, and the continuation wave field is:

$$\begin{aligned} P(\tau,\omega) = P(0,\omega)\exp\left[\int_0^{\tau}\left(\frac{\omega}{\omega_{\mathrm{h}}}\right)^{-r(\tau')}\frac{\omega}{2Q(\tau')}\mathrm{d}\tau'\right] \\ \times\exp\left[-j\int_0^{\tau}\left(\frac{\omega}{\omega_{\mathrm{h}}}\right)^{-r(\tau')}\omega\,\mathrm{d}\tau'\right] \end{aligned} \tag{4}$$

Further deformation (4),

$$\begin{aligned} P(\tau,\omega) = P(0,\omega)\Lambda(0,\omega) \\ \times\exp\left[-j\int_0^{\tau}\left(\frac{\omega}{\omega_h}\right)^{-r(\tau)'}\omega\,\mathrm{d}\tau'\right] \end{aligned} \tag{5}$$

$$\Lambda(\tau,\omega) = \frac{\beta(\tau,\omega)+\sigma^2}{\beta^2(\tau,\omega)+\sigma^2} \tag{6}$$

$$\beta(\tau,\omega) = \exp\left[-\int_0^{\tau}\left(\frac{\omega}{\omega_h}\right)^{-r(\tau')}\frac{\omega}{2Q(\tau')}\mathrm{d}\tau'\right] \tag{7}$$

where, σ^2 is a stability factor, which is related to the gain limit of the actual data $G_{\lim}$(db),

$$\sigma^2 = \exp[-(0.23G_{\lim} + 1.63)] \tag{8}$$

In order to improve the efficiency of inverse Q filtering, the Gabor transform is used to inverse Q filtering in time and frequency domain, and then the formula (4) is changed to,

$$\begin{aligned} P(\tau,\omega) &= \tilde{P}(\tau,\omega)\Lambda(\tau,\omega) \\ &\quad\times \exp\left[-j\int_0^{\tau}\left(\left(\frac{\omega}{\omega_{\mathrm{h}}}\right)^{-r(\tau')} - 1\right)\omega\,\mathrm{d}\tau'\right] \end{aligned} \tag{9}$$

where, $\tilde{P}(\tau,\,\omega) = P(0,\omega)\exp[j\omega\tau]$

Formula (9) is an inverse Q filter equation based on Gabor transform. For the wave field of different time depth, the surface seismic record is transformed by Gabor, and the amplitude compensation operator and phase compensation operator are combined to carry out inverse Q filtering in time and frequency domain. The inverse Gabor transform can be used to obtain the seismic record $P(t)$ via inverse Q filtering for the obtained wave field $P(\tau,\omega)$.

4 Spectral Decomposition Technique Represented by Generalized *S* Transformation

The time series $h(t) \in L^2(R)$, $L^2(R)$ represent the integrable function space on the real number field. The S transformation proposed by Stockwell can be expressed as follows.

$$S(\tau,f) = \int_{-\infty}^{\infty} h(t)\left\{\frac{|f|}{\sqrt{2\pi}}\exp\left[\frac{-f^2(\tau-t)^2}{2}\right]\right\}\mathrm{d}t \quad \int_{-\infty}^{\infty}\exp(-\mathrm{i}2\pi ft)\mathrm{d}t \tag{10}$$

where, τ,f denote time and frequency respectively, both are real numbers. The basic wavelets $w(t)$ in the S transform are

$$w(t) = \frac{\lambda|f|^{2a}}{\sqrt{2\pi}}\exp\left[\frac{-\lambda^2 f^{2a}(\tau-t)^2}{2}\right]\exp(-\mathrm{i}2\pi ft) \tag{11}$$

Then the generalized S transformation is obtained.

$$\mathrm{GST}(\tau,f) = \int_{-\infty}^{\infty} h(t)\left\{\frac{\lambda|f|^{2a}}{\sqrt{2\pi}}\exp\left[\frac{-\lambda^2 f^{2a}(\tau-t)^2}{2}\right]\right\}\mathrm{d}t \times \int_{-\infty}^{\infty} \exp(-\mathrm{i}2\pi ft)\mathrm{d}t \quad (12)$$

Although wavelet transform (WT) can realize multi-scale focusing, the relationship between wavelet scale and frequency is uncertain. The generalized S transform inherits the advantages of STFT and WT transform and overcomes their disadvantages: The time window in low-frequency section is wider and the frequency resolution is higher, the time window in high-frequency section is narrower, and the time resolution is very high.

5 Spectral Shaping Technology

The amplitude of a given seismic record is corrected to make it a specified form, which usually the amplitude spectrum is 1 at a given frequency, and the amplitude spectrum is a smaller value outside the given frequency. Transforming the seismic record into the frequency domain by Fourier transform to calculate the amplitude spectrum, and weighting the amplitude spectrum to correct according to the amplitude-frequency, while keeping the phase spectrum unchanged, then the spectral shaping record is obtained by inverse Fourier transform.

Although the amplitude spectrum shaping technique is the most commonly used spectrum adjustment technology, there are some problems: For all components in the frequency correction, noise may be amplified; plastic spectrum is defined by the user, and there are many artificial control factors. Spectrum shaping technology can be used before and after stack. The specific prestack or poststack application depends on the quality of the collected data. Because both the low frequency and high frequency are easy to weaken and the frequency band is narrower during the processing, so the distribution of effective frequency needs to be adjusted.

6 Viscoelastic Prestack Time Migration Technique

Viscoelastic prestack time migration technique is the characteristic technology of independent intellectual property of Daqing Institute, which uses the equivalent Q rather than the exact Q value when describing the dissipation of seismic waves. The seismic wave propagation time is calculated using equivalent velocity (root mean square velocity) rather than layer equation of wave field continuation in inhomogeneous viscous media can be velocity. On the basis of these two equivalent parameters, the analytical obtained. Using each seismic data as a collection of data, a viscoelastic medium backpropagation channel is obtained through a one-way travel from the surface to the deep layer,

$$\mathrm{P}^{U}(x,y,\omega,T)=F(\omega)\frac{\omega}{2\pi}\exp\left(-j\frac{\pi}{2}\right)\frac{T}{\tau_{\mathrm{g}}^{2}V_{\mathrm{rms}}^{2}}\times\exp\left\{j\omega\tau_{\mathrm{g}}\left[1-\frac{1}{\pi\mathrm{Q}_{\mathrm{e}}}\ln\left(\frac{\omega}{\omega_{0}}\right)\right]\right\}\exp\left(\frac{\omega\tau_{\mathrm{g}}}{2Q_{\mathrm{e}}}\right)\tag{13}$$

where, τ_{g} is the travel time of the elastic medium at the receiving point to the imaging point (x, y, T), $F(\omega)$ is the Fourier transform of seismic trace, V_{rms} and Q_{e} are the two equivalent parameters introduced for this paper, where

$$V_{\mathrm{rms}}=\sqrt{\frac{1}{T}\sum_{l=1}^{n}V_{l}\Delta T_{l}},\quad\frac{1}{Q_{\mathrm{e}}}=\frac{1}{T}\sum_{l=1}^{n}\frac{\Delta T_{l}}{Q_{l}}\tag{14}$$

V_{rms} corresponds to the root mean square velocity of the regular time offset an Q_{e} is the equivalent Q value corresponding to the imaging point space position. In formula (13), two terms related to Q_{e} represent dispersion and amplitude attenuation caused by dielectric absorption, and the fourth is the influence of geometric diffusion of wave propagation. The forward wave source wave field is as follows,

$$P^{D}(x,y,\omega,T)=\frac{S(\omega)\omega}{2\pi}\exp\left(j\frac{\pi}{2}\right)\frac{T}{\tau_{\mathrm{s}}^{2}V_{\mathrm{rms}}^{2}}\exp\left(-\frac{\omega\tau_{\mathrm{s}}}{2Q_{\mathrm{e}}}\right)\times\exp\left\{-j\omega\tau_{\mathrm{s}}\left[1-\frac{1}{\pi Q_{\mathrm{e}}}\ln\left(\frac{\omega}{\omega_{0}}\right)\right]\right\}\tag{15}$$

$S(\omega)$ is Fourier transformation in seismic wavelet. In formula (13) and formula (15), τ_g and τ_{s} are the propagation time in elastic medium, which can be obtained by the detection point and the lateral coordinates of the seismic source. Although formulas (13) and formula (15) are derived under the assumption of layered media, the propagation of waves in a lateral inhomogeneous medium can be dealt with only by allowing V_{rms} and Q_{e} transversal changes.

From formula 13 and formula 15, we can see that the frequency-dependent travel time (the second exponential term in the formula) and amplitude compensation factor, as well as the amplitudes from the detection point and the source propagation to the imaging point, are determined only by the imaging point V_{rms} and Q_{e}. In this way, the two equivalent parameters can be determined by scanning method.

Like the traditional prestack time migration, the Kirchhoff compensation algorithm is used to compensate the medium absorption prestack time migration. However, the formula for compensating viscous medium absorption prestack time bias imaging conditions derived by Zhang Jianfeng et al., which is obtained by prestack depth migration, that is, each seismic trace is treated as a shot set. We use formula (13) and formula (15) to propagate seismic traces backward and forward propagation of source wave field in depth domain using one-way travel time T. Because the influence of the source wavelet can be eliminated by deconvolution. We neglected the first three items $S(\omega)[\omega/2\pi]\exp(j\pi/2)$ of the wave field in the formula (13). The formula (16) is obtained by substituting the forward propagating source wave field and the backward propagating seismic trace the into the prestack depth migration deconvolution imaging condition.

$$I(x,y,T) = \left(\frac{\tau_s}{\tau_g}\right)^2 \int F(\omega)\frac{\omega}{2\pi}\exp(-j\frac{\pi}{2})\mathrm{d}\omega \times \int \left\{\left[1 - \frac{1}{\pi Q_e}\ln\left(\frac{\omega}{\omega_0}\right)\right]\right\}\exp\left[\frac{\omega(\tau_s+\tau_g)}{2Q_e}\right]\mathrm{d}\omega \int \exp\{j\omega(\tau_s+\tau_g)\mathrm{d}\omega \tag{16}$$

Formula (16) represents the migration pulse response of a seismic trace. The migration result is obtained by summing the impulse response of all seismic traces. Different from the conventional prestack time migration, the frequency-dependent dispersion term and amplitude compensation term (Q_e related binomial) are introduced into the frequency domain formula. When Q_e approaches infinity, the frequency integral in formula (16) is simplified to estimate the first order time derivative of seismic trace at the time $\left(\tau_g + \tau_s\right)$.

Formula (16) is simplified to conventional prestack time migration. The CRP gather can be obtained by calculating and summing the pulse response of each seismic trace. This is similar to conventional prestack time migration. The appropriate migration aperture should be set in advance and determined by the maximum dip angle of the formation at different times to be imaged. Two equivalent parameters V_{rms} and Q_e are required for viscoelastic prestack time migration. The velocity parameter V_{rms} can be obtained by establishing a conventional prestack time migration velocity model. Equivalent parameter Q_e can be obtained by scanning the equivalent Q parameter. In order to obtain Q model from ground seismic data, another problem must be dealt with, that is, thin layer tuning effect caused by thin interlamination. The strong tuning effect results in the occurrence of notch frequency in the reflected wave spectrum, and the error Q value can be obtained by using the spectral ratio method or the frequency shift method directly. The equivalent scanning method uses multiple constant Q viscoelastic prestack time migration results and picks up the best Q value. In order to reduce the computational workload of constant Q migration, we simplify formula (16) to constant Q formula, so that viscoelastic prestack time migration is simplified as prestack inverse Q filter plus constant Q model prestack time migration.

Stability is a problem faced by all kinds of absorption compensation algorithms. Only by solving the stability problem and noise suppression problem of absorption compensation in medium and deep layers can we obtain the absorption compensation of the actual data in the middle and deep layers. This is because the amplitude compensation factor (the last term on the right of formula (16) approaches infinity for smaller travel times and higher frequencies. Because the prestack time migration for compensating viscous absorption has obtained an analytical compensation factor, we can ensure that when the compensation factor is less than the specified gain limit, the function is completely consistent with the accurate amplitude compensation factor by setting a smoothing gain function. The gain limit value is gradually approaching. The gain function is as follows,

$$\phi(\eta) = \exp(\eta), \quad \eta \leq \ln G \tag{17}$$

$$\begin{aligned}\phi(\eta) = {} & G(1 - \ln G - 2.5(\ln G)^2) \\ & + G(1 + 5\ln G)\eta - 2.5G\eta^2, \quad \ln G < \eta < \ln G + 0.2\end{aligned} \tag{18}$$

$$\phi(\eta) = 1.1G, \quad \eta > \ln G + 0.2 \tag{19}$$

where, $\eta = \omega(\tau_g + \tau_s)/(2Q_e)$ denotes gain limitation and stable imaging results can be obtained by using amplitude compensation factor $\exp\{\omega(\tau_g + \tau_s)/(2Q_e)\}$ in $\varphi(\eta)$ instead of formula (16).

By comparing several techniques to improve the resolution, it can be seen that the inverse Q filter is not enough to protect the low frequency, and the low-frequency deficiency of the processing result is serious, but the low-frequency component is the key to the prediction of dense-gas desserts. The spectral decomposition technique is difficult to control the frequency spectrum shape of the high-frequency end, it is easy to raise too high and reduce the high-frequency signal-to-noise ratio, and the spectrum shaping technology expects that the output spectrum will have more artificial control factors to be easily controlled. According to the characteristics and potential of the data, the fidelity and amplitude-preserving frequency can be maximized, and the technology of prestack time migration for viscoelastic media is advanced and effective, but it cannot meet the requirements of large area industrialization in a short period of time. By comparing and analyzing the principle, the improved method of spectrum shaping as the main frequency extension technique is adopted to improve the resolution of seismic data in the study area.

7 Example

The research base of deep unconventional reservoir prediction is seismic data with wideband amplitude-preserving processing. In order to improve the fidelity and amplitude preservation, the characteristic processing techniques, such as iterative noise suppression and 3D Q compensation, are adopted. In order to improve the imaging accuracy of deep complex structures, a velocity model is established by using high precision mesh chromatography. By using prestack depth domain inverse time migration (CIG) focusing imaging technique, there is abundant information among the layers of the section after migration, the relationship between wave groups is clear, and the section is clear about fracture points, which is beneficial to the development of poststack frequency extension processing.

Based on this data, (1) comprehensive spectrum analysis is carried out for the target layer; (2) the spectrum analysis of the whole region after the anti-Q filter is analyzed; (3) the amplitude spectrum and phase spectrum of the output anti-Q filter are output; (4) the result of step (3) is done by inverse Fourier transform to get the global statistical wavelet one after the anti-Q filtering; (5) by using the method of statistical amplitude spectrum energy envelope, the results of step (1) and step (2) are used to obtain the expected output wavelet 2 by inverse Fourier transform, and the global filter operator is obtained by shaping wavelet 2. By convolution between the operator and the seismic data after anti-Q filtering, the final results are obtained. The above is the spectral shaping technique flow based on global statistical wavelet.

It can be seen from Fig. 2 that this method not only improves the high frequency, but also keeps the low-frequency feature well, and the main frequency and the octave of the data are increased simultaneously. The global filtering operator of this method is based on global data statistics, and it does not change the relative amplitude relation, so it is amplitude preserving. After increasing the frequency, the main frequency of seismic profile is increased by 14 Hz, the resolution is improved significantly, the information between layers is abundant, the matching degree of synthetic records is improved, and the imaging clarity of the four-level sequence interface is slightly improved. From the comparison of Fig. 3, it can be seen that the amplitude attribute characteristics are similar and the amplitude distribution characteristics are consistent before and after spectral shaping, which proves the amplitude preservation of this technique

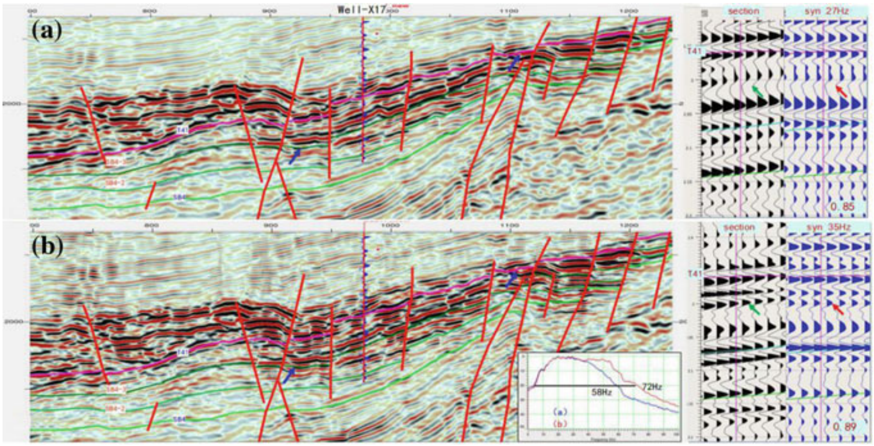

Fig. 2. Comparison of profile contrast before and after spectral shaping and matching degree of synthetic records

In the geological model of phase control guiding ideology, comprehensive analysis using multiple attribute recognition gradually sandstone area: (1) The high-frequency reflection areas of shallow lake facies or marsh facies developed in coal seam and thin sandstone are excluded by high value of frequency attributes; (2) the amplitude of high value further eliminate the thick coal seam (>2 m) compared with the developed areas and the front sub thick dry layer sandstone area; (3) low impedance attribute values exclude the prodelta mudstone interbedded with thin siltstone of low-frequency weak amplitude and low impedance reflection area. Through correlation analysis, we choose the instantaneous bandwidth attributes and peak amplitude attributes which have good correlation with lithology and lay a foundation for qualitative prediction of sandstone relative development area. Comprehensive analysis of the following two properties for

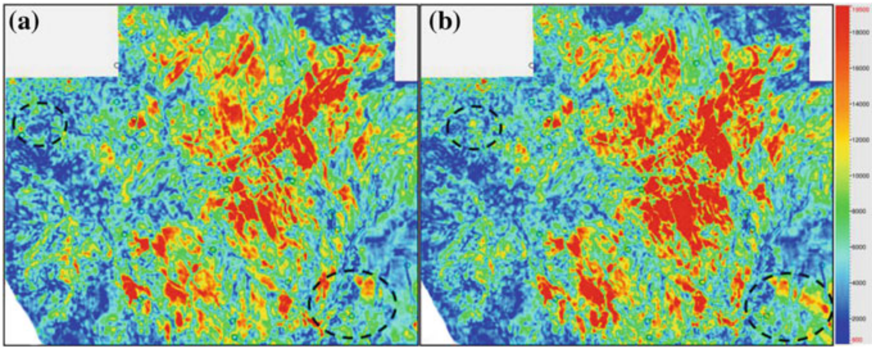

Fig. 3. **a** Before the spectral shaping, the SB4-3 root mean square amplitude property slice and **b** the SB4-3 root mean square amplitude property slice after spectral shaping

favorable sedimentary facies identification are: (1) The high value of instantaneous bandwidth properties excludes the development area of coal seam, middle and low value identification front and plain facies sandstone development area; (2) the peak amplitude attribute can distinguish between the leading edge coherent sandstone and the gas-bearing sandstone development zone, the middle-high value corresponds to the dry sand development area, the middle and low value corresponds to the gas sand development area, the peak amplitude attribute corresponds to the very developing area of the coal seam, in which the lithological assemblage is mainly composed of thick mudstone, coal seam and thin siltstone, and a thicker coal seam with a single layer thickness of over 2 m is developed. On this basis, combined with the relative wave impedance inversion results of no well constraints, the favorable area of sandstone is predicted. The reason is that the mean property of the relative wave impedance can distinguish between the plain and the front deltaic thick mudstones which are indistinguishable from the instantaneous and peak amplitude properties.

The final criteria for determining the unconventional tight sandstone gas desserts in the area are: instantaneous bandwidth—low value, peak amplitude attribute—low value, and high value in relative impedance. Under the guidance of this knowledge, the sandstone undeveloped area is gradually eliminated with multi-attribute synthesis, and the favorable development area of sandstone is predicted and the multiple solution of single attribute prediction is reduced. The coincidence rate is raised from 67 to 80%. In the statistics of 14 wells, the coincidence rate of SQ4-3 is 85%, the average coincidence rate of the 7 layer statistics in SQ4-SQ2 sequence is 80%. As can be seen from Fig. 4, Fig. 4a is the seismic section of well X34 in the post well, and Fig. 4b is the relative wave impedance section of the over well. The relative wave impedance inversion of X34 well predicts 8 layers of sandstone. The real drilling meets 8 layers of sandstone, in which there are 3 layers of sand formation and 3 layers of more than 10 m single sand. The relative inversion prediction accords with 6 layers (2 layers of single sand body, 4 layers of sand layer), and the inversion prediction coincidence rate is 75%. The SQ4-2 layer (No. 36 layer) sand ratio is 0.47. The range of blue brackets in the three attribute figures (Fig. 4c is instantaneous bandwidth property, Fig. 4d is peak amplitude property, Fig. 4e is relative impedance inversion) that predict a favorable area for dessert, and the prediction results reveal the development of sandstone, consistent with the real drilling.

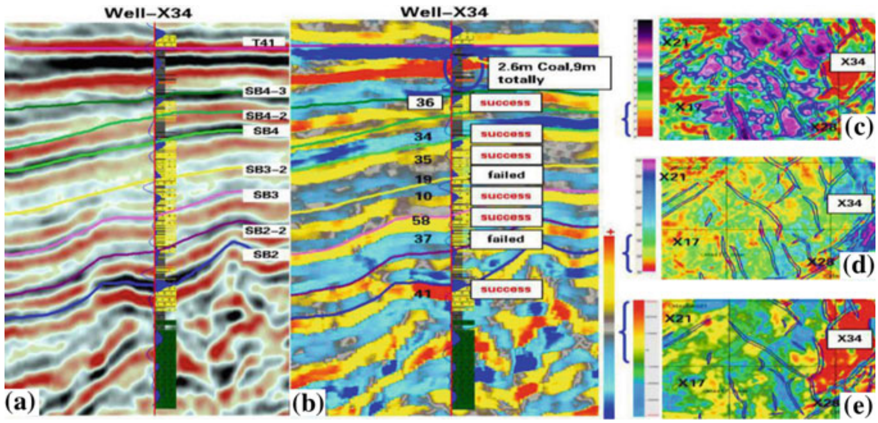

Fig. 4. **a** Cross-well seismic profile, **b** relative impedance inversion section, **c** instantaneous bandwidth attribute diagram, **d** peak amplitude attribute diagram and **e** relative impedance inversion plane map

8 Conclusions

(1) According to the principle and the applicable conditions, the spectral shaping method is optimized to improve the vertical resolution of seismic data. Using the wavelet based on global statistics without changing the relative amplitude relation, the frequency processing has the amplitude-preserving property. After the process, the main frequency of the data is increased by 14 Hz, and the definition of the four sequence interface is improved. Improving high frequency and keeping low frequency, the main frequency and octave frequency range are increased simultaneously, and the seismic true resolution is improved.

(2) The detailed full attribute analysis is carried out on the basis of spectral shaping extension data to optimize the property of instantaneous bandwidth and peak amplitude with better correlation with lithology, which lays the foundation for the qualitative prediction of sandstone relative development zone. The mean property of the relative wave impedance can distinguish between the plain thick layer sand conglomerate and the front delta thick mudstone which cannot be distinguished from the instantaneous and peak amplitude properties. Finally, the multi-attribute comprehensive analysis combined with the relative impedance inversion strategy is used to predict the dessert of the deep dense gas.

(3) The new processing results are optimized by combining multi-attribute and relative wave impedance inversion to select the “dessert area” of sandstone, which reduces the multi-solution of single attribute prediction. The average coincidence rate is increased from 67 to 80%. The prediction coincidence rate of sand body inversion in X34 well is 75%, and the prediction coincidence rate of SQ4-3 sequence sandstone is 85.7%.

(4) Spectral shaping and frequency expansion technology based on wideband amplitude-preserving imaging processing support the location deployment of 7 exploration wells in the area and provide strong technical support for increasing storage and production in unconventional fields. Multi-attribute comprehensive analysis combined with the method of relative impedance inversion has high prediction accuracy of deep dense gas and has a good prospect of popularization and application.

References

1. Gao JH, Chen WC, Li YM, et al. Generalized S transformation and seismic response of thin interbeds. Chin J Geophys. 2003;46(4):526–532.
2. Gao JH, Man W, Chen SM. Recognition of signals from colored noise background in generalized S-transform domain. Chin J Geophys. 2004;75(5):869–75.
3. Wan H, Fan XY, Liu T, et al. Methods and applications for improving pre-stack seismic data resolution. Prog Geophys. 2012;27(1):304–11 (in Chinese).
4. Li ZC, Wang QZ. A review of research on mechanism of seismic attenuation and energy compensation. Prog Geophys. 2007;22(4):1147–52.
5. Yao ZX, Gao X, Li WX. The forward *Q* method for compensating attenuation and frequency dispersion used in the seismic profile for depth domain. Chin J Geophys. 2003;46(2):229–33.
6. Hargreaves ND, Calvert AJ. Inverse *Q*-filtering by Fourier transform. Geophys. 1991;56 (4):519–27.
7. Wang YH. A stable and efficient approach of inverse *Q* filtering. Geophys. 2002;67(2):657–63.
8. Hale D. An inverse *Q*-filter. Stanford Explor Project. 1981;28:289–98.
9. Chen CR, Zhou XX. Improving resolution of seismic data using wavelet spectrum whitening. Oil Geophys Prospect. 2000;35(6):703–9.
10. Stockwell RG, Mansinha L, Lower RP. Localization of the complex spectrum: the S-transform. IEEE Trans Signal Process. 1996;44(4):998–1001.
11. Liu XW, Liu H, Li YM, et al. Study on characteristics of seismic stratigraphyized S-transform. Prog Geophys. 2006;21(2):440–51.
12. Pinnegar CR, Mansinha L. The S-transform with windows of arbitrary and varying shape. Geophys. 2003;68(1):381–5.
13. Pinnegar CR, Eaton DW. Application of S transform to prestack noise attenuation filtering. J Geophys Res. 2003;108(B9):1–10.
14. Zhang GL, Xiong XJ, Rong JJ, et al. Stratum absorption and attenuation compensation based on improved generalized S-transform formation. Oil Geophys Prospect. 2010;45(4):512–5.
15. Li GF, Zhou H, Zhou H, Zhao C. Potential risks of spectrum whitening deconvolution-compared with well-driven deconvolution. Pet Sci. 2009;6:146–52.

16. Mauricio DS, Danilo RV, Alberta HC. Minimum entropy deconvolution with frequency-domain constraints. Geophys. 1994;59(6):938–45.
17. Lu PF, Yang CC, Guo AH. The present research on frequency-spectrum imaging technique. Prog Geophys. 2007;22(5):1517–21.

Author Biography

Yi Bao male, Master of Engineering, Exploration and Development Research Institute of Daqing Oilfield Company Ltd. CNPC, engineer. The research field is seismic data processing, processing and interpretation integration, complex structure imaging, etc.